HHS Public Access

Author manuscript

J Cardiovasc Transl Res. Author manuscript; available in PMC 2015 October 01.

Published in final edited form as:

J Cardiovasc Transl Res. 2013 February ; 6(1): 54–64. doi:10.1007/s12265-012-9428-x.

Murine Cytomegalovirus (MCMV) Infection Upregulates P38 MAP kinase in Aortas of Apo E KO Mice: a Molecular Mechanism for MCMV-Induced Acceleration of Atherosclerosis

Yajarayma J. Tang-Feldman,
Department of Internal Medicine, University of California, Davis, Sacramento, CA 95817, USA

Stephanie R. Lochhead,
Department of Internal Medicine, University of California, Davis, Sacramento, CA 95817, USA

G. Raymond Lochhead,
Department of Internal Medicine, University of California, Davis, Sacramento, CA 95817, USA

Cindy Yu,
Department of Pathology, University of California, Davis, Sacramento, CA 95817, USA

Michael George,
Department of Medical Microbiology and Immunology, University of California, Davis, Sacramento, CA 95817, USA

Amparo C. Villablanca, and
Department of Internal Medicine, University of California, Davis, Sacramento, CA 95817, USA

Claire Pomeroy
Department of Internal Medicine, University of California, Davis, Sacramento, CA 95817, USA. Department of Internal Medicine and Department of Medical Microbiology and Immunology, University of California, Davis, Sacramento, CA 95817, USA

Yajarayma J. Tang-Feldman: yjtangfeldman@ucdavis.edu; Claire Pomeroy: claire.pomeroy@ucdmc.ucdavis.edu

Abstract

Multiple studies suggest an association between cytomegalovirus (CMV) infection and atherogenesis; however, the molecular mechanisms by which viral infection might exacerbate atherosclerosis are not well understood. Aortas of MCMV-infected and uninfected Apo E knockout (KO) mice were analyzed for atherosclerotic lesion development and differential gene expression. Lesions in the infected mice were larger and showed more advanced disease compared to the uninfected mice. Sixty percent of the genes in the MAPK pathway were upregulated in the infected mice. p38 and ERK 1/2 MAPK genes were 5.6- and 2.0-fold higher, respectively, in aortas of infected vs. uninfected mice. Levels of VCAM-1, ICAM-1, and MCP-1 were ~2.0–2.6-fold higher in aortas of infected vs. uninfected mice. Inhibition of p38 with SB203580 resulted in lower levels of pro-atherogenic molecules and MCMV viral load in aortas of infected mice.

Correspondence to: Claire Pomeroy, `claire.pomeroy@ucdmc.ucdavis.edu`.

Electronic supplementary material The online version of this article (doi:10.1007/s12265-012-9428-x) contains supplementary material, which is available to authorized users.

MCMV-induced upregulation of p38 may drive the virus-induced acceleration of atherogenesis observed in our model.

Keywords

MCMV; Atherosclerosis; MAPK; p38; ERK1/2; Inflammation

Introduction

Atherosclerosis is a chronic multifactorial inflammatory disease of the vascular system and the major cause of myocardial infarction and stroke. The initial steps of atherosclerosis involve the accumulation of monocytes from the circulation in the subendothelial layer followed by differentiation of monocytes into macrophages. Macrophage uptake of oxidized low density lipids (oxLDL) leads to the formation of foam cells. The products of these cells (cytokines, chemokines, and growth factors) constitute fatty streaks, the earliest atherosclerotic lesions. Local vascular production of cytokines, chemokines, and growth factors contributes to the subsequent local inflammatory response resulting in the formation of atherosclerotic lesions [1–3].

CMV is a β-herpes virus for which there is evidence of previous infection in 40–95 % of adults worldwide. Primary human CMV (HCMV) infection is followed by a lifelong persistence of the virus in a latent state in the immunocompetent host; subclinical reactivation occurs frequently leading to a chronic and probably intermittent viremic state. Host responses to HCMV infection are characterized by the production of pro-inflammatory cytokines (including TNF-α, IFN-γ, and IL-6) which correlate with severity of the disease and with viral loads [4–6]. Even though there is accumulating evidence suggesting an association between HCMV infection and atherogenesis [7–9] the role of HCMV in atherosclerosis is controversial. HCMV DNA has been detected in atherosclerotic lesions, and it has been suggested that HCMV is a possible etiologic co-factor in the atherosclerotic process [10–12]. Despite these findings, the molecular mechanisms underlying this association are not well understood. HCMV infection triggers activation of many transcription factors in the host including mitogen-activated protein kinases (MAPK). MAPK are cellular signaling kinases that activate numerous transcription factors. Three major groups of MAPK are identified: ERK1/2, p38, and JNK. HCMV infection induces expression of host p38 and ERK1/2 which results in increased viral replication [13–15]. It has been shown that HCMV infection alters the p38 and ERK1/2 MAPK pathways by attenuating cellular phosphatases resulting in prolonged activation of these kinases [15]. Phosphorylation of these genes is essential for HCMV gene expression. Activation of p38 and ERK 1/2 affects downstream transcription factors including activator protein 1 (AP-1). AP-1 upregulates macrophage migration inhibitory factor (MIF) promoting foam cell formation and secretion of pro-inflammatory mediators (cytokines and chemokines) involved in atherogenesis [16, 17].

The goal of this study was to determine the impact of CMV infection on atherogenesis and to define molecular pathways/cellular genes altered by the virus which are relevant in

atherosclerosis. We hypothesized that MCMV infection accelerates atherosclerosis by activating the MAPK gene, p38, leading to an increase in pro-inflammatory, pro-atherosclerotic molecules, and foam cell formation.

Materials and Methods

Mice

Pathogen-free female 5–6-week-old Apo E KO (C57BL/6 background) mice were purchased from Jackson Laboratories (Bar Harbor, ME, USA). Pathogen-free female 5–6-week-old wild type (WT) C57BL/6 were obtained from Harlan-Sprague–Dawley (Indianapolis, IN, USA), and were used as the WT (baseline) strain in the DNA microarray studies. All mice were housed in American Association for Assessment and Accreditation of Laboratory Animal Care-approved specific pathogen-free facility at our institution and had free access to food and water. Mice were fed a standard diet (PicoLab Mouse Diet 5058, Purina Lab Diet, Framingham, MA). Animal studies and protocols were approved by the University of California, Davis Institutional Animal Care and Use Committee.

Virus and Infection

The Smith strain of MCMV was obtained from the American Type Culture Collection (Manassas, VA, USA) and maintained by salivary gland passage in BALB/c mice. Salivary gland homogenates were prepared in RPMI 1640 (Gibco Laboratories, Grand Island, NY, USA) as previously described [18]. The sublethal dose to establish a clinical infection was determined using standard protocols [18]. Mice were infected intraperitoneally (i.p.) with a sublethal dose containing ~10^5 plaque forming units (PFU) of MCMV as determined by the plaque assay. At 4 and 8 weeks post-infection, mice were challenged with a sub-clinical dose containing ~10^3PFU of MCMV to mimic CMV reactivation. In all studies, control (uninfected) mice received the same volume (0.2 ml) of RPMI i.p. at the designated time points. RVG-102, a recombinant MCMV derived from the Smith strain and expressing enhanced green fluorescence protein (EGFP) [19] was kindly provided by Dr. J. Shanley. The recombinant virus was used in experiments to visualize the presence of MCMV in atherosclerotic lesions. RVG-102 was propagated by salivary gland passage as described above. To determine if viable MCMV was required for acceleration of atherosclerosis lesion development, an inactivated MCMV was prepared by UV irradiation as described [20]. No viable plaque forming units were detected using the plaque assay after three rounds of viral irradiation (10 min each). A group of Apo E KO mice was infected and challenged with the inactivated MCMV as described above for the viable MCMV. UV-killed (inactivated) MCMV was only used in the DNA microarray studies to compare mRNA expression profile in aortas of mice infected with live MCMV vs. killed MCMV.

Nucleic Acid Extraction and cDNA Synthesis

Two and a half months after infection, groups of mice were killed by terminal anesthesia and hearts perfused with phosphate-buffered saline. Aortas from MCMV-infected and uninfected Apo E KO mice (n=10 for each) were microscopically dissected and placed in nucleic acid purification lysis solution (Applied Biosystems, Foster City, CA, USA) for RNA extraction. RNA extraction and cDNA synthesis were performed at the Molecular

Core Facility, School of Veterinary Medicine at our institution using a 6700 RNA extraction apparatus (Applied Biosystems, Foster City, CA, USA). DNA from aortas was extracted with the DNeasy Blood and Tissue kit (Qiagen, Valencia, CA, USA) following the manufacturer's instructions.

Real-Time Polymerase Chain Reaction (qRT-PCR) of Adhesion Molecules

Transcription profiles of the adhesion molecules ICAM-1 and VCAM-1 and of MCP-1, as well as transcription of the housekeeping genes GAPDH and HPRT were determined by quantitative real-time PCR (qRT-PCR) using gene expression assay kits (Applied Biosystems) with the respective primers/fluorogenic probe mix specific for each gene. qRT-PCR reactions were set up in duplicate for each gene. Amplification conditions were identical and consisted of 2 min at 50 °C, 10 min at 95 °C, 40 cycles of 15 s at 95 °C, and 60 s at 60 °C. Final quantification was performed using the comparative C_T method as described [5, 21]. Briefly, for each experimental sample, the difference between the target C_T value and the C_T value of the most stable housekeeping gene for each tissue type was used to normalize for differences in the amount of total nucleic acid added to each reaction, and the efficiency of the RT step (ΔC_T). For relative quantification by the comparative C_T method, values are expressed relative to a reference sample, called the calibrator, which is the weakest signal from the normalized values or ΔC_T. The ΔC_T from each aorta sample was subtracted from the ΔC_T of the calibrator ($\Delta\Delta C_T$). The amount of target (linear value) normalized to an internal control or housekeeping gene and relative to the calibrator was determined by $2^{\Delta\Delta C_T}$. The linear value represents the linear expression of each gene in infected mice minus that in uninfected mice.

Quantification of MCMV DNA in Aortas

MCMV DNA was quantified in aortas as previously described [5]. Amplification and cloning of the immediate early gene 1 (IE1), sequences of the primers and fluorogenic probe, amplification conditions, and final quantification are described elsewhere [5].

Assessment of Atherosclerotic Lesions in the Aorta of MCMV-Infected vs. Uninfected Apo E KO Mice

At 2.5 months after infection, mice were sacrificed by terminal anesthesia, the hearts exposed and perfused with PBS and aortas dissected free from the aortic arch to the iliac bifurcation, and trimmed of external fat. Aortas were then embedded in OCT compound, and 7-μm thick sections were cut consecutively on a Leica CM3050 cryostat at −20 °C and placed on a SuperPlus Frost microscopic slide (Fisher Scientific, Pittsburgh, PA, USA) and stored at −80 °C until ready for histologic staining with H&E. Atherosclerotic lesions in the aortic root (proximal segment), mid segment (proximal to the renal arteries), and distal aorta (proximal to the iliac bifurcation) were visualized with Oil Red O stain (ORO). Lesion analysis was performed by a trained pathologist blinded to the treatment of the mice. Lesion areas were quantified with the Axio Vision computer software (Carl Zeiss, New York, NY, USA) and expressed as square micrometers.

RNA Isolation, Microarray Hybridization, and Microarray Analysis

RNA was extracted from aortas of Apo E KO mice infected with a live MCMV, a UV-killed MCMV, and from uninfected control mice at the Molecular Core Facility, School of Veterinary Medicine at our institution using the Qiagen RNeasy extraction kit (Qiagen). Amplification and labeling of mRNA was performed using the Ovation© RNA amplification kit and Encore Biotin© module (NuGEN Technologies, Inc., San Carlos, CA). Hybridization to Mouse Genome 430 2.0 GeneChip© arrays (Affymetrix, Santa Clara, CA), staining, and scanning were carried out according to protocols in the Affymetrix Gene Expression Analysis Technical Manual. Analyses of microarray data were performed using dChip (http://biosun1.harvard.edu/complab/dchip/) software. A minimum 2.0-fold difference between groups (p value≤0.05) was used as criteria for identifying differentially expressed genes. Pathway analysis of differentially expressed genes was accomplished using The Database for Annotation, Visualization and Integrated Discovery (DAVID) v6.7 [22, 23] and Ingenuity Pathway Analysis software. The entire microarray data set is deposited at the Gene Expression Omnibus at the National Center for Biotechnology Information.

Validation of p38 Differential Gene Expression by RT-PCR and Western Blot

Quantitative real-time PCR was used to confirm differential gene transcription of p38 and ERK1/2 in aortas of MCMV-infected (live) and uninfected control Apo E KO mice. Gene-specific primers and fluorogenic probes for p38 and ERK 1/2 were obtained from Applied Biosystems (inventoried primer/probe kits). qRT-PCR and analyses of data were performed as described above for adhesion molecules. For Western blot studies, proteins from aortas of MCMV-infected (n=5) and uninfected Apo E KO mice (n=5) were extracted using the Qiagen Q proteome Cell Compartment kit (Qiagen) following the manufacturer's instructions. Protein quantity was determined spectrophotometrically at 260 nm. Twelve percent polyacrylamide Mini-PROTEAN TGX gels for SDS-PAGE electrophoresis were obtained from BIO RAD (Hercules, CA, USA). Protein samples (~13 μg) were loaded per well. Biotinylated Protein Ladder (Cell Signaling Technology, Danvers, MA, USA) was loaded in two lanes of the gels for size markers. Samples were transferred to a PVDF membrane (BIO RAD) and subjected to Western blot analysis. Membranes were incubated with a rabbit monoclonal phospho-p38 MAPK antibody (Cell Signaling Technology, #4511) overnight at 4 °C, then subjected to incubation with a horseradish peroxidase-linked anti-rabbit secondary antibody (Cell Signaling Technology) for 1 h at room temperature. Detection of protein was performed using LumiGLO reagents (Cell Signaling Technology) on a Kodak Image Station 4000 MM PRO (Carestream Health Inc., Rochester, NY, USA). Analysis was done using the Carestream Molecular Imaging Software. Protein fold-increase was the average of five samples for the infected and five samples for the uninfected Apo E KO mice.

Visualization of Green Fluorescence Protein (gfp)-Labeled MCMV and of Co-localization with p38 in Atherosclerotic Lesions

For detection of gfp-MCMV, samples of aorta were embedded in OCT compound (VWR Scientific, San Francisco, CA, USA) and stored at −80 °C until ready to section. Consecutive sections (5 μm) were cut on a cryostat and mounted on positively charged

slides as described above. Sections were visualized under standard fluorescence microscopy. Visualization of p38 and gfp-MCMV in atherosclerotic lesions was done using a phospho-p38 MAPK mouse monoclonal antibody (mAb) to the phosphorylated form of the protein (Thr 180/Tyr 182; Cell Signaling Technology #9216S) and an anti-gfp rabbit mAb, respectively (Cell Signaling Technology) incubated at 4 °C overnight. Samples were then incubated with an anti-mouse IgG conjugated to Alexa-Fluor 555 and an anti-rabbit IgG conjugated to Alexo-Fluor 488 (Cell Signaling Technology) for 1 h at room temperature. Prolong Gold Anti-fade reagent with DAPI for nuclear staining (Invitrogen, Carlsbad, CA, USA) was placed on all sections, and sections were cover-slipped. Slides were visualized on a Nikon E800 fluorescence microscope in conjunction with the Q-Capture Pro software (Nikon, Melville, NY, USA).

p38 Inhibition Studies

In studies designed to confirm the role of p38 activation in atherogenesis and MCMV replication, MCMV-infected Apo E KO mice were treated with the p38 inhibitor SB203580-HCL (EMD Biosciences, Hayward, CA). Briefly, mice were treated with 50 mg/kg of the inhibitor via intraperitoneal injection 15 min after MCMV infection and every 8 h thereafter, for 24 h. After four treatments with SB203580, mice (n=8) were sacrificed, aortas dissected, and analyzed for MCMV DNA viral load; mRNA expression levels of p38, ICAM-1, VCAM-1, and MCP-1; and pro-inflammatory cytokines (IL-1α, IL-1β, IL-6, IFN-γ, and TNF-α) using real-time PCR. Assays were performed in duplicate on aortas from eight mice per time point. Control mice included: a group of MCMV-infected, untreated Apo E KO mice, and uninfected-p38 inhibitor treated Apo E KO mice.

Statistical Analyses

Statistically significant differences in mRNA transcription profile in aortas of MCMV-infected and uninfected Apo E KO mice were determined using the Student t test with significance defined as $p \leq 0.05$. For DNA microarray analyses, a minimum 2.0-fold difference between groups was used as criteria for identifying differentially expressed genes. Data was analyzed using the dChip software.

Results

Differential mRNA Expression in Aortas of Apo E KO Mice Compared to WT, C57BL/6 Mice

Differences in mRNA expression patterns in aortas of Apo E KO mice and the WT, C57BL/6 mice were determined by DNA microarray analysis. Genes that were differentially expressed were categorized according to their functional activity and/or metabolic pathways. Significant differences were identified in the expression profile of aortas from Apo E KO mice compared to the wild type in genes involved in immune response (T-cell differentiation, lymphocyte activation, innate immune response, and B-cell receptor signaling pathway) and inflammatory pathways (Supplemental Figure 1). In contrast, genes associated with regulation of neurogenesis, hormone activity, and mitotic cell cycle were downregulated in aortas of Apo E KO vs. the WT, C57BL/6.

Transcriptional Profiles at Early Stages of Atherosclerosis in Aortas of MCMV-Infected (live and UV-killed) vs. Uninfected Apo E KO Mice

To identify genes altered by MCMV infection, and those that may be involved in viral-induced acceleration of atherogenesis, we analyzed transcriptional profiles in aortas from Apo E KO mice infected with live MCMV and with UV-killed MCMV compared to uninfected Apo E KO mice and the WT, C57BL/6, at 2.5 months after infection. Aortas of Apo E KO mice infected with live MCMV showed upregulation of all (100 %) the studied genes (included in the microarray chip) involved in T-cell differentiation, innate immune response, lymphocyte activation, B-cell receptor signaling, and inflammatory responses (Fig. 1a and d), while only 60–80 % of genes in these categories were induced in uninfected mice (Fig. 1b) or mice infected with a UV-killed MCMV (Fig. 1c). Infection with live MCMV also resulted in significant changes in the expression of genes in the mitogen-activated protein kinase and interferon-gamma-related pathways. Sixty percent of the genes in these pathways were upregulated by infection with live MCMV compared to only about 40 % of genes in mice infected with UV-killed or uninfected mice. Among the genes in the MAPK pathway, p38 and ERK 1/2 showed over 2-fold increases in the aortas of mice infected with live MCMV vs. those infected with UV-killed MCMV or uninfected mice. We therefore chose to study these two genes in further depth, as they are known to be involved in both MCMV viral gene expression and in atherogenesis. Because no significant difference in expression of the MAP kinase genes of interest was observed between the mice infected with the UV-killed MCMV and the uninfected controls, no further molecular experiments were performed with the UV-killed MCMV.

Over-Expression of p38 mRNA in Aortas of MCMV-Infected Apo E KO Mice at 2.5 Months Post-Infection

Because of the significant upregulation shown in the DNA microarray analysis of p38 and ERK 1/2 MAPK genes, we validated the results using quantitative real-time PCR (qRT-PCR) in aortas from MCMV-infected and uninfected Apo E KO mice (n=10 each). Expression of mRNA transcripts of p38 and ERK 1/2 averaged ~5.6-fold and ~2-fold higher (p<0.01), respectively, in aortas of MCMV-infected Apo E KO compared to uninfected mice at 2.5 months post-infection (Fig. 2a). p38 was activated in aortas of both MCMV-infected and uninfected mice, but by Western blot analysis MCMV-infected mice showed a ~1.7-fold increase in phosphorylated p38 levels compared to uninfected mice (Fig. 2b). There was no significant difference in levels of activated ERK1/2 between the infected and uninfected mice (data not shown).

MCMV-Induced Upregulation of p38 MAP Kinase Results in Elevated Transcript Levels for ICAM-1, VCAM-1, and MCP-1 in Aortas of Apo E KO Mice

MCMV infection of Apo E KO mice was associated with elevated transcription levels of adhesion molecules known to be involved in the atherosclerotic process. Levels of transcripts for the adhesion molecules ICAM-1 and VCAM-1, and of MCP-1 were 2-fold (p=0.008), 2.5-fold (p=0.001), and 2.2-fold (p<0.05) higher, respectively, in aortas of MCMV-infected compared to uninfected Apo E KO mice (Fig. 2). Serum levels of IFN-γ were ~4.5-fold higher (p<0.05) in MCMV-infected Apo E KO mice (average of 27.6 vs. 6

pg/ml in uninfected mice). We also observed a trend toward an increase in levels of other pro-inflammatory cytokines (IL-1α and IL-1β) in the MCMV-infected vs. uninfected mice (data not shown).

Inhibition of p38 Results in Downregulation of Adhesion Molecules (ICAM-1, VCAM-1), MCP-1, Pro-Inflammatory Cytokines, and a Reduction of MCMV DNA Viral Load in Aortas

Inhibition of p38 MAP kinase following four treatments with the p38 inhibitor SB203580 resulted in a significant decrease in mRNA levels of VCAM-1 and MCP-1 but not ICAM-1 (Fig. 3a). mRNA levels of VCAM-1, MCP-1, and ATF-2, a downstream signaling factor, were 2-, 3.5-, and 1.5-fold lower, respectively, in aortas of SB203580 treated compared to untreated mice ($p<0.05$). We also observed significant decreases in the pro-inflammatory cytokines IFN-γ and TNF-α in aortas of MCMV-infected, p38 inhibitor-treated Apo E KO mice compared to MCMV-infected, untreated mice (Fig. 3b). Viral load in aortas of the treated mice were 12-fold lower after four treatments with the p38 inhibitor (Fig. 3c). No significant difference in transcription levels of genes in the ERK1/2 pathway (c-Raf, MEK1/2, and ERK1/2) was observed in aortas of mice treated with SB203580 or untreated mice (Supplemental Figure 2).

Detection of gfp-MCMV and Co-Localization of p38 and MCMV in Atherosclerotic Lesions of MCMV-Infected Apo E KO Mice

In order to determine the presence of MCMV in atherosclerotic lesions, we used a recombinant MCMV expressing EGFP (RVG-102). We detected localized areas of fluorescence in atherosclerotic lesions of Apo E KO mice infected with RVG-102 (Fig. 4a–c). No fluorescence was observed in atherosclerotic lesions from uninfected mice, as expected (data not shown). To further confirm that the fluorescence observed was due to gfp-MCMV, an anti-gfp antibody was used in co-localization studies of gfp-MCMV and p38. A monoclonal antibody specific to p38 was used to identify p38 in atherosclerotic lesions. As shown in Fig. 5, gfp-MCMV and p38 were detected and co-localized in aortic lesions of MCMV-infected Apo E KO mice. Using qRT-PCR, MCMV DNA (175 IE1 gene copies/100 mg of aorta) was also detected in aortas of the infected mice (data not shown).

MCMV Infection Accelerates Atherosclerotic Lesion Progression in Aortas of Apo E KO Mice

Quantification of lesion area in the aortic valves and aortic arch revealed a significant increase in lesion size in MCMV-infected Apo E KO mice compared to uninfected mice. At 2.5 months after infection, total lesion area in the aortic valve leaflets was ~30 % greater in the infected vs. uninfected Apo E KO mice ($p=0.03$; Fig. 6c). Characterization of lesions demonstrated that MCMV-infected Apo E KO mice had more advanced lesions compared to uninfected mice or mice infected with the UV-killed MCMV of the same age (Fig. 6a–c). Atherosclerotic lesions were also observed in the mid aortic segment of 60 % of the MCMV-infected but not in the uninfected Apo E KO mice (data not shown).

In our studies, MCMV infection had no effect on serum cholesterol or triglycerides levels. Cholesterol (548±77 mg/DL) and triglycerides (104±18 mg/DL) levels in MCMV-infected

mice were comparable to those in uninfected mice (597±174 and 135±62 mg/DL for cholesterol and triglycerides, respectively; $p>0.1$).

Discussion

Using transcriptional profiling of genes in aortas of MCMV-infected vs. uninfected Apo E KO mice, we demonstrate that (1) MCMV infection accelerates lesion development early during atherogenesis; (2) MCMV infection upregulates genes in the host mitogen activated protein kinase pathway, specifically p38, which is used for viral genome replication; and (3) upregulation of p38 promotes foam cell formation and expression of pro-inflammatory, pro-atherosclerotic molecules resulting in acceleration of atherosclerosis. These data provide new insights into molecular mechanisms involved in CMV-induced acceleration of atherosclerosis.

The role of CMV infection in cardiovascular disease has been controversial. Results from a population-based study evaluating cardiovascular risk factors and seropositivity to various pathogens [24] showed that antibody titers against CMV were not a marker for prevalence or incidence of atherosclerosis. However, evidence from animal studies points to an active role of CMV in cardiovascular disease including atherosclerosis [12, 25–30]. It has been suggested that the contribution of CMV to atherosclerosis is through the initiation and sustainment of inflammatory processes [26–28] induced by the virus. In a review on CMV and cardiovascular disease, Stassen et al. [30] suggested that besides inflammation, other processes such as autoimmunity due to cross-reactivity between human and viral proteins, may exacerbate atherosclerosis.

Despite these numerous studies addressing a link between CMV infection and atherogenesis, the molecular mechanisms underlying this association are not completely understood. In this study, we present evidence that one of the mechanisms by which MCMV infection accelerates atherosclerosis is through activation of the mitogen-activated protein kinase pathway, specifically p38 MAP kinase. p38 MAP kinase is essential for and plays an important role in the efficiency of HCMV DNA replication [13, 15, 31]. CMV infection upregulates transcription of MAP kinases in host tissues resulting in increased viral genome expression and viral replication. We found significant upregulation of p38 in aortas of MCMV-infected vs. uninfected Apo E KO mice. Furthermore, immunostaining of sections of aortas of gfp-MCMV-infected Apo E KO mice with antibodies to phosphorylated p38 showed co-localization of MCMV and p38 in atherosclerotic lesions at 2.5 months after infection. In concert with MCMV-induced upregulation of p38 MAP kinase, levels of adhesion molecules (ICAM-1 and VCAM-1) and MCP-1 were significantly elevated in atherosclerotic lesions of the infected mice, and these lesions were larger, more complex, and more advanced in infected compared to uninfected Apo E KO mice.

We found that mice infected with UV-killed MCMV had elevated mRNA expression of some of the genes in the MAPK and immune response pathways analyzed in our DNA microarray system, suggesting that viral proteins/antigens might also activate these pathways. It is likely that continuous MCMV antigen exposure may be a contributing factor in atherogenesis. These observations are supported by the studies of Vliegen et al. [29] in

which infection with a UV-inactivated MCMV was found to increase T-cell numbers in atherosclerotic lesions as did infection with viable MCMV. These authors suggested that MCMV infection may aggravate atherosclerosis via an immune-mediated effect and that autoimmunity could be involved in this process. In our study, we did not observe a significant difference in lesions size in the mice infected with a UV-inactivated MCMV vs. uninfected mice, possibly due to the different time points and age of the mice used in the two studies.

Among the multiple roles that p38 plays in cardiovascular disease are: stimulation of cell migration and proliferation, upregulation of expression of MCP-1 attracting monocytes to the endothelium, differentiation of monocytes to macrophages, and endothelial migration [32–34]. More recently, Mei et al. [35] reported a direct role for p38 in foam cell formation through promoting cholesterol ester accumulation and inhibiting autophagy [35]. Johnson et al. [15] showed that p38 is activated for extended periods of time after HCMV infection and that phosphorylation of p38 is essential for CMV replication and completion of the viral life cycle. These authors demonstrated that one of the mechanisms by which HCMV induces prolonged activation of p38 is by inhibition of dephosphorylation of p38. Our data showed that inhibition of p38 with the p38 inhibitor SB203580-HCL resulted in reduced MCMV viral load in aortas of infected mice. We did not find activation of the Raf-MEK-ERK pathways in aortas of SB203580 treated mice as has been reported by others [36]. These differences may be due to the experimental approach and methodology of both studies (mouse Swiss 3T3 fibroblasts and human 293 cells in the study of Hall-Jackson et al. [36] vs. our *in vivo* studies of atherosclerotic lesions in Apo E KO mice). Our results imply that p38 may be one of the predominant pathways used by MCMV for replication as is the case with HCMV.

The decline in MCMV in aortas of p38 inhibitor treated mice was associated with downregulation of mRNA expression of pro-inflammatory cytokines (IL-1-α, IL-1β, IL-6, IFN-γ, TNF-α, and IL-6) and the adhesion molecules ICAM-1, VCAM-1, and also MCP-1, p38, and downstream transcription factor ATF-2. In support of our results, p38 inhibitors have been shown to inhibit TNF-α and collagen-induced arthritis in mice and rat models [37]. The p38 MAPK pathway plays a major role in inflammatory processes and in the development of inflammatory disorders and diseases (Crohn’s disease, rheumatoid arthritis, chronic inflammation, and chronic obstructive pulmonary disease) including atherosclerosis [37–39]. p38 MAP kinase is also required for platelet-derived growth factor-induced cell responses such as aortic endothelial cell migration [40]. The data presented in this study strongly suggest that upregulation of p38 MAP kinase is one of the molecular mechanisms involved in MCMV-induced acceleration of atherosclerosis, and that this pathway may be a useful target for therapeutic development for both CMV infection and atherosclerosis.

A limitation of our study is that the Apo E KO model may not reflect the process of atherogenesis in wild-type mice (or humans). However, this model has been well studied to understand the fundamental mechanisms of atherogenesis. Another limitation is that microarray analysis identified a number of candidate genes to study. Our results identified the MAPK pathway as important, but future studies are planned to assess additional candidate genes which may play a role. Also, the co-localization of p38 and gfp-MCMV in

lesions does not prove a causative role; however, the studies documenting a SB203580-induced decrease in pro-inflammatory mediators suggests a potential biologic basis for the accelerated plaque formation. Longer-term studies of p38 blockade may provide additional evidence.

Despite these limitations, the results presented in this study have significant clinical implications and suggest a potentially important role of signaling pathways in atherosclerosis, including the possibility that co-stimulation of these pathways aggravates the atherogenic process. Importantly, we identified genes that are involved in atherosclerosis and thus may be potential therapeutic targets for prevention and intervention of atherosclerotic disease. A number of drugs which inhibit these pathways are already available, and our studies provide a foundation for designing human therapeutic trials.

Collectively, our findings demonstrate that MCMV infection activates p38 MAP kinase resulting in over-expression of downstream transcription factors such as ATF-2, one of the components of activator protein-1 (AP-1). Activation of AP-1 leads to upregulation of macrophage inhibitory factor (MIF) which promotes foam cell formation and secretion of pro-inflammatory, pro-atherogenic mediators (cytokines and chemokines) involved in atherogenesis [16, 34, 35].

In conclusion, these studies provide new insights into a molecular mechanism linking CMV infection, MAPK pathway, inflammation, and atherosclerosis. We propose the following as one of the mechanism by which MCMV infection accelerates atherosclerosis: atherosclerotic lesions are primarily composed of LDL-rich macrophages and monocytes both of which are target cells infected by MCMV. These MCMV-infected cells travel from the circulation to the vascular endothelium where they adhere; once leukocyte migration occurs, there is viral upregulation of host MAPK proteins with subsequent induction of leukocyte adhesion molecules (ICAM-1, VCAM-1). These molecular events lead to increased and accelerated foam cell and fatty streak formation with progression of atherosclerosis including the development of more advanced and complex plaque lesions.

Taken together, our results suggest that MCMV infection contributes to atherosclerosis by modulating genes in host pathways which are involved both in viral replication and in atherogenesis. Prolonged activation of p38 is one of the molecular mechanisms by which MCMV infection may accelerate progression of atherosclerosis. Further studies are in progress in our laboratory to define differences in gene profiling patterns at different stages of atherosclerosis in MCMV-infected Apo E KO mice. Our studies provide the basis for exploring treatment of CMV to limit atherosclerosis, either directly with antivirals or by modulation of the inflammatory mediators induced by the virus.

Supplementary Material

Refer to Web version on PubMed Central for supplementary material.

Acknowledgments

The authors thank the Lucy Whittier Molecular Core Facility at the School of Veterinary Medicine, UC Davis, for excellent technical assistance with the RNA extraction and cDNA synthesis. We are grateful to Mr. Matthew Rolston at the UC Davis School of Medicine DNA Microarray Core Facility for assistance with the DNA microarray analyses.

This work was supported in part by an Innovative Development Award (YTF) from UC Davis Academic Federation and by grant UL1 RRO24146 from the National Center for Research Resources (NCRR), a component of the National Institutes of Health (NIH) and NIH Road Map for Medical Research (CP), and the Frances Lazda Endowment in Women's Cardiovascular Medicine (ACV).

References

1. Ross R. The pathogenesis of atherosclerosis: a perspective for the 1990s. Nature. 1993; 362:801–809. [PubMed: 8479518]
2. Glass CK, Witztum JL. Atherosclerosis. The road ahead. Cell. 2001; 104:503–516. [PubMed: 11239408]
3. Hansson GK, Libby P. The immune response in atherosclerosis: a double-edged sword. Nature Reviews Immunology. 2006; 6:508–519.
4. Orange JS, Biron CA. Characterization of early IL-12, IFN-alphabeta, and TNF effects on antiviral state and NK cell responses during murine cytomegalovirus infection. Journal of Immunology. 1996; 156:4746–4756.
5. Tang-Feldman YJ, Wojtowicz A, Lochhead GR, Hale MA, Li Y, Pomeroy C. Use of quantitative real-time PCR (qRT-PCR) to measure cytokine transcription and viral load in murine cytomegalovirus infection. Journal of Virological Methods. 2006; 131:122–129. [PubMed: 16140399]
6. Ritter JT, Tang-Feldman YJ, Lochhead GR, Estrada M, Lochhead S, Yu C, et al. In vivo characterization of cytokine profiles and viral load during murine cytomegalovirus-induced acute myocarditis. Cardiovascular Pathology. 2010; 19:83–93. [PubMed: 19217318]
7. Blum A, Giladi M, Weinberg M, Kaplan G, Pasternack H, Laniado S, et al. High anti-cytomegalovirus (CMV) IgG antibody titer is associated with coronary artery disease and may predict post-coronary balloon angioplasty restenosis. The American Journal of Cardiology. 1998; 81:866–868. [PubMed: 9555776]
8. Grattan MT, Moreno-Cabral CE, Starnes VA, Oyer PE, Stinson EB, Shumway NE. Cytomegalovirus infection is associated with cardiac allograft rejection and atherosclerosis. Journal of the American Medical Association. 1989; 261:3561–3566. [PubMed: 2542633]
9. Espinola-Klein C, Rupprecht HJ, Blankenberg S, Bickel C, Kopp H, Victor A, et al. Impact of infectious burden on progression of carotid atherosclerosis. Stroke. 2002; 33:2581–2586. [PubMed: 12411646]
10. Hendrix MG, Dormans PH, Kitslaar P, Bosman F, Bruggeman CA. The presence of cytomegalovirus nucleic acids in arterial walls of atherosclerotic and nonatherosclerotic patients. American Journal of Pathology. 1989; 134:1151–1157. [PubMed: 2541613]
11. Zhou YF, Guetta E, Yu ZX, Finkel T, Epstein SE. Human cytomegalovirus increases modified low density lipoprotein uptake and scavenger receptor mRNA expression in vascular smooth muscle cells. The Journal of Clinical Investigation. 1996; 98:2129–2138. [PubMed: 8903333]
12. Hsich E, Zhou YF, Paigen B, Johnson TM, Burnett MS, Epstein SE. Cytomegalovirus infection increases development of atherosclerosis in Apolipoprotein-E knockout mice. Atherosclerosis. 2001; 156:23–28. [PubMed: 11368993]
13. Rodems SM, Spector DH. Extracellular signal-regulated kinase activity is sustained early during human cytomegalovirus infection. Journal of Virology. 1998; 72:9173–9180. [PubMed: 9765464]
14. Johnson RA, Ma XL, Yurochko AD, Huang ES. The role of MKK1/2 kinase activity in human cytomegalovirus infection. Journal of General Virology. 2001; 82:493–497. [PubMed: 11172089]

15. Johnson RA, Huong SM, Huang ES. Activation of the mitogen-activated protein kinase p38 by human cytomegalovirus infection through two distinct pathways: a novel mechanism for activation of p38. Journal of Virology. 2000; 74:1158–1167. [PubMed: 10627526]
16. Hu Y, Cheng L, Hochleitner BW, Xu Q. Activation of mitogen-activated protein kinases (ERK/JNK) and AP-1 transcription factor in rat carotid arteries after balloon injury. Arteriosclerosis, Thrombosis, and Vascular Biology. 1997; 17:2808–2816.
17. Fledderus JO, van Thienen JV, Boon RA, Dekker RJ, Rohlena J, Volger OL, et al. Prolonged shear stress and KLF2 suppress constitutive proinflammatory transcription through inhibition of ATF2. Blood. 2007; 109:4249–4257. [PubMed: 17244683]
18. Pomeroy C, Hilleren PJ, Jordan MC. Latent murine cytomegalovirus DNA in splenic stromal cells of mice. Journal of Virology. 1991; 65:3330–3334. [PubMed: 1851880]
19. Henry SC, Schmader K, Brown TT, Miller SE, Howell DN, Daley GG, et al. Enhanced green fluorescent protein as a marker for localizing murine cytomegalovirus in acute and latent infection. Journal of Virological Methods. 2000; 89:61–73. [PubMed: 10996640]
20. Heise MT, Virgin HW. The T-cell-independent role of gamma interferon and tumor necrosis factor alpha in macrophage activation during murine cytomegalovirus and herpes simplex virus infections. Journal of Virology. 1995; 69:904–909. [PubMed: 7815559]
21. Kipar A, Leutenegger CM, Hetzel U, Akens MK, Mislin CN, Reinacher M, et al. Cytokine mRNA levels in isolated feline monocytes. Veterinary Immunology and Immunopathology. 2001; 78:305–315. [PubMed: 11292531]
22. da Huang W, Sherman BT, Lempicki RA. Systematic and integrative analysis of large gene lists using DAVID bioinformatics resources. Nature Protocols. 2009; 4:44–57. [PubMed: 19131956]
23. da Huang W, Sherman BT, Lempicki RA. Bioinformatics enrichment tools: paths toward the comprehensive functional analysis of large gene lists. Nucleic Acids Research. 2009; 37:1–13. [PubMed: 19033363]
24. Mayr M, Kiechl S, Willeit J, Wick G, Xu Q. Infections, immunity, and atherosclerosis: associations of antibodies to *Chlamydia pneumoniae*, *Helicobacter pylori*, and cytomegalovirus with immune reactions to heat-shock protein 60 and carotid or femoral atherosclerosis. Circulation. 2000; 102:833–839. [PubMed: 10952949]
25. Leskov IL, Whitsett J, Vasquez-Vivar J, Stokes KY. NAD(P)H oxidase and eNOS play differential roles in cytomegalovirus infection-induced microvascular dysfunction. Free Radical Biology & Medicine. 2011; 51:2300–2308. [PubMed: 22033010]
26. Burnett MS, Durrani S, Stabile E, Saji M, Lee CW, Kinnaird TD, et al. Murine cytomegalovirus infection increases aortic expression of proatherosclerotic genes. Circulation. 2004; 109:893–897. [PubMed: 14757699]
27. Vliegen I, Stassen F, Grauls G, Blok R, Bruggeman C. MCMV infection increases early T-lymphocyte influx in atherosclerotic lesions in apoE knockout mice. Journal of Clinical Virology. 2002; 25(Suppl 2):S159–S171. [PubMed: 12361766]
28. Vliegen I, Duijvestijn A, Stassen F, Bruggeman C. Murine cytomegalovirus infection directs macrophage differentiation into a pro-inflammatory immune phenotype: implications for atherogenesis. Microbes and Infection. 2004; 6:1056–1062. [PubMed: 15380774]
29. Vliegen I, Herngreen SB, Grauls GE, Bruggeman CA, Stassen FR. Mouse cytomegalovirus antigenic immune stimulation is sufficient to aggravate atherosclerosis in hypercholesterolemic mice. Atherosclerosis. 2005; 181:39–44. [PubMed: 15939052]
30. Stassen FR, Vega-Cordova X, Vliegen I, Bruggeman CA. Immune activation following cytomegalovirus infection: more important than direct viral effects in cardiovascular disease? Journal of Clinical Virology. 2006; 35:349–353. [PubMed: 16387544]
31. Chen Y, Currie RW. Heat shock treatment suppresses angiotensin II-induced SP-1 and AP-1 and stimulates Oct-1 DNA-binding activity in heart. Inflammation Research. 2005; 54:338–343. [PubMed: 16158334]
32. Goebeler M, Kilian K, Gillitzer R, Kunz M, Yoshimura T, Brocker EB, et al. The MKK6/p38 stress kinase cascade is critical for tumor necrosis factor-alpha-induced expression of monocyte-chemoattractant protein-1 in endothelial cells. Blood. 1999; 93:857–865. [PubMed: 9920834]

33. Marin V, Farnarier C, Gres S, Kaplanski S, Su MS, Dinarello CA, et al. The p38 mitogen-activated protein kinase pathway plays a critical role in thrombin-induced endothelial chemokine production and leukocyte recruitment. Blood. 2001; 98:667–673. [PubMed: 11468165]

34. Domoto K, Taniguchi T, Takaishi H, Takahashi T, Fujioka Y, Takahashi A, et al. Chylomicron remnants induce monocyte chemoattractant protein-1 expression via p38 MAPK activation in vascular smooth muscle cells. Atherosclerosis. 2003; 171:193–200. [PubMed: 14644387]

35. Mei S, Gu H, Ward A, Yang X, Guo H, He K, et al. p38 mitogen-activated protein kinase (MAPK) promotes cholesterol ester accumulation in macrophages through inhibition of macroautophagy. Journal of Biological Chemistry. 2012; 287:11761–11768. [PubMed: 22354961]

36. Hall-Jackson CA, Goedert M, Hedge P, Cohen P. Effect of SB 203580 on the activity of c-Raf in vitro and in vivo. Oncogene. 1999; 18:2047–2054. [PubMed: 10321729]

37. Badger AM, Bradbeer JN, Votta B, Lee JC, Adams JL, Griswold DE. Pharmacological profile of SB 203580, a selective inhibitor of cytokine suppressive binding protein/p38 kinase, in animal models of arthritis, bone resorption, endotoxin shock and immune function. Journal of Pharmacology and Experimental Therapeutics. 1996; 279:1453–1461. [PubMed: 8968371]

38. Hollenbach E, Neumann M, Vieth M, Roessner A, Malfertheiner P, Naumann M. Inhibition of p38 MAP kinase- and RICK/NF-kappaB-signaling suppresses inflammatory bowel disease. The FASEB Journal. 2004; 18:1550–1552. [PubMed: 15289440]

39. Renda T, Baraldo S, Pelaia G, Bazzan E, Turato G, Papi A, et al. Increased activation of p38 MAPK in COPD. European Respiratory Journal. 2008; 31:62–69. [PubMed: 17959643]

40. Matsumoto T, Yokote K, Tamura K, Takemoto M, Ueno H, Saito Y, et al. Platelet-derived growth factor activates p38 mitogen-activated protein kinase through a Ras-dependent pathway that is important for actin reorganization and cell migration. Journal of Biological Chemistry. 1999; 274:13954–13960. [PubMed: 10318806]

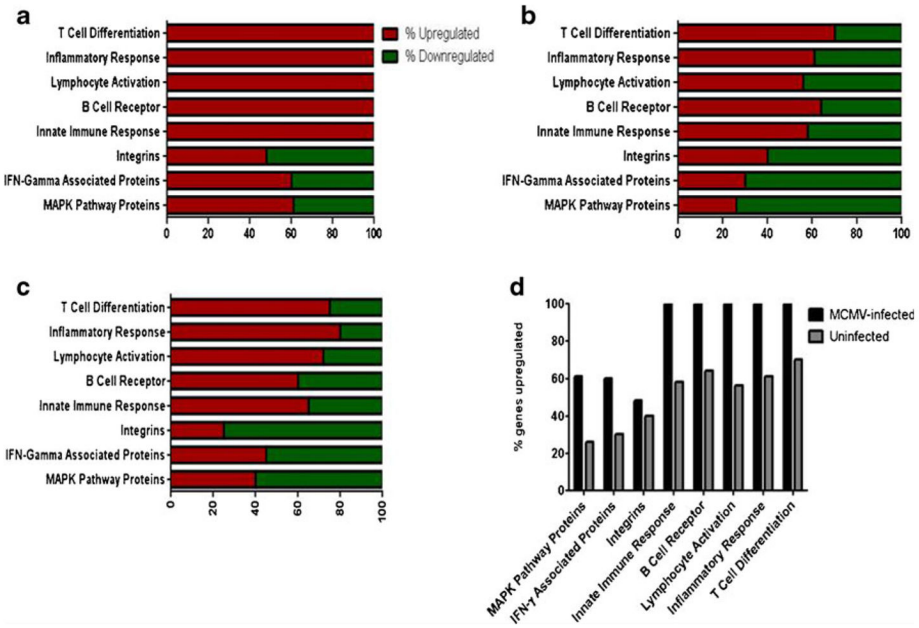

Fig. 1.

Percent of genes up/downregulated in aortas Apo E KO mice (MCMV-infected, UV-killed MCMV-infected, and uninfected) vs. wild-type C57BL/6 at 2.5 months post-infection. **a** MCMV-infected Apo E KO mice vs. wild-type C57BL/6; **b** uninfected control vs. wild-type C57BL/6; **c** UV-killed MCMV-infected vs. wild-type C57BL/6; **d** MCMV-infected vs. uninfected Apo E KO mice

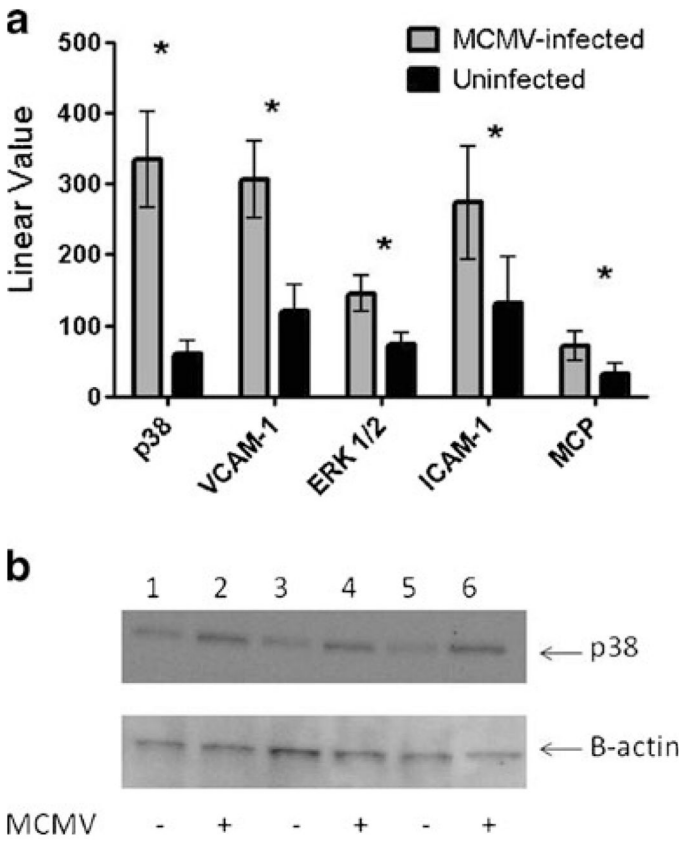

Fig. 2.

mRNA transcripts in aortas of MCMV-infected vs. uninfected Apo E KO mice (value is average of *n*=10 mice) at 2.5 months post-infection. **a** Real-time PCR was performed on cDNA using primers/fluorogenic probes specific for each gene and analysis done as described in "Materials and Methods" section; **b** validation of phosphorylated p38 expression by Western blot at 2.5 months post-infection: *lanes 1, 3, and 5* protein patterns from aortas of uninfected Apo E KO mice; *lanes 2, 4, and 6* protein patterns from aortas of MCMV-infected Apo E KO mice. Figure is representative of *n*=5 MCMV-infected and five uninfected control Apo E KO mice. Average levels of phosphorylated p38 protein were ~1.7-fold higher in aortas from MCMV-infected vs. uninfected Apo E KO mice. Significance (*) at $p \leq 0.05$

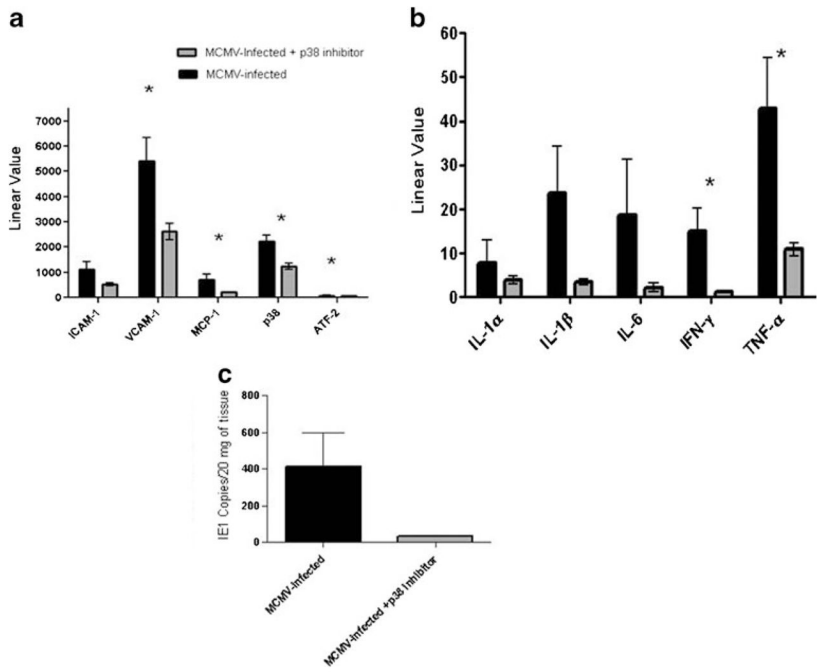

Fig. 3.

Effect of p38 inhibitor, SB203580, on pro-atherogenic molecules and MCMV viral loads in aortas of MCMV-infected Apo E KO mice. **a** mRNA levels of adhesion molecules, MCP-1, p38, and ATF-2 in aortas of MCMV-infected, SB203580-treated vs. untreated mice; **b** mRNA levels of pro-inflammatory cytokines in aortas of MCMV-infected, SB203580-treated vs. untreated mice; **c** MCMV IE1 gene copies in aortas of MCMV-infected, SB203580-treated vs. untreated mice. Mice were treated four times, every 8 h for 24 h with SB203580. Values are average of n=10 mice per group. Significance (*) at $p \leq 0.05$

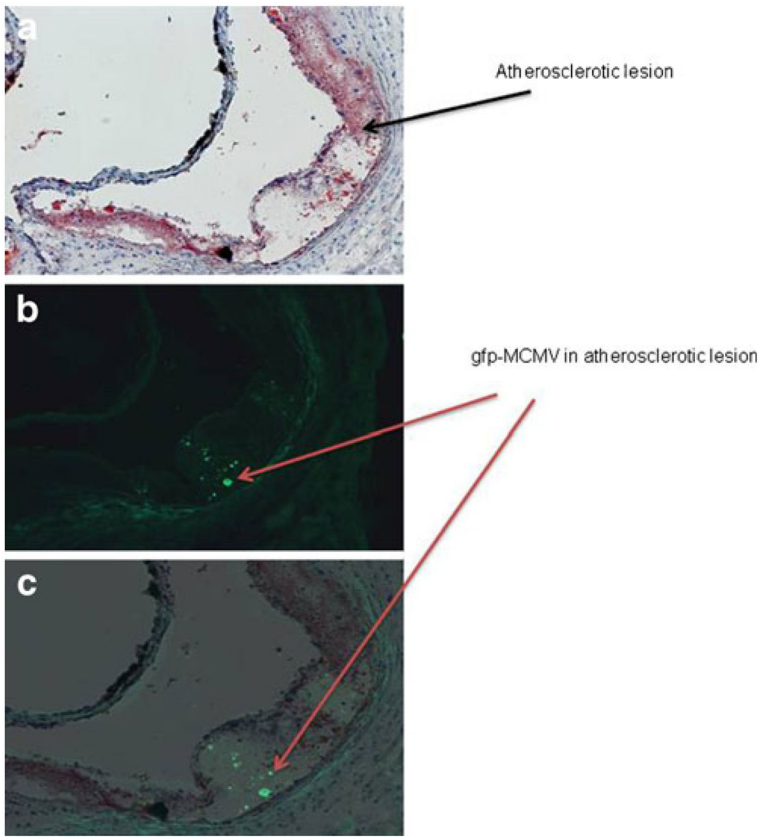

Fig. 4.

Atherosclerotic lesions in aortas of gfp-MCMV-infected Apo E KO mice at 2.5 months post-infection. **a** Lipid ORO-stained section; **b** consecutive section under fluorescence microscopy; **c** section B superimposed over section A, showing localization of GFP staining in the atherosclerotic plaque. Magnification ×20

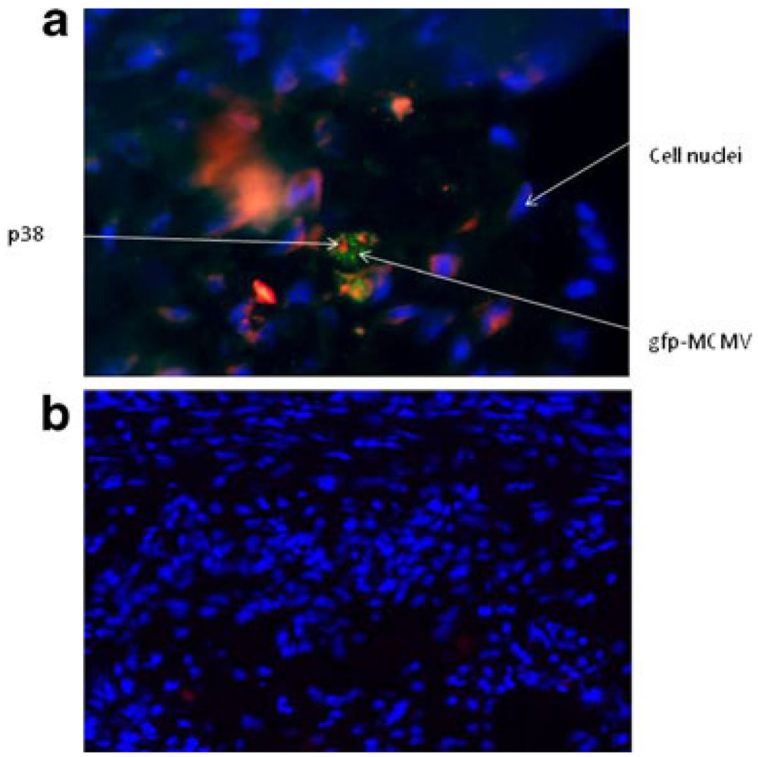

Fig. 5.

Co-localization of gfp-labeled MCMV and p38 in atherosclerotic lesions (figure is representative of eight samples). **a** Cross-section of an aorta showing an atherosclerotic lesion in a MCMV-infected Apo E KO mouse. MCMV is labeled with gfp (*green*), p38 with Alexafluor 555 (*red*), and nuclei with DAPI (*blue*). Magnification is ×100; **b** cross-section of an aorta showing an atherosclerotic lesion in an uninfected mouse stained as in (**a**). Note that only DAPI-stained nuclei are observed (magnification is ×40)

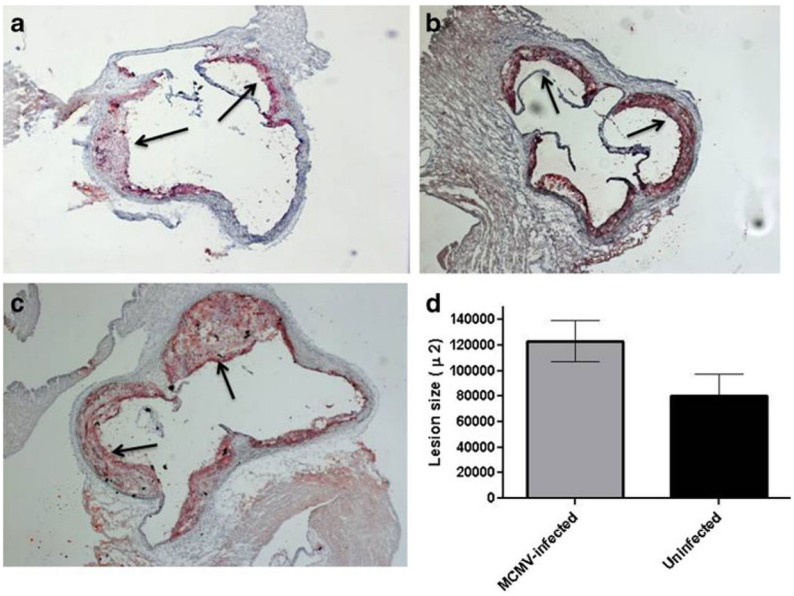

Fig. 6.

Representative figures of atherosclerotic lesions in aortic sinus of MCMV-infected and uninfected Apo E KO mice at 2.5 months post-infection. **a** Lesions in aortas of uninfected mice (*n*=8); **b** lesions in aortas of mice infected with a UV-killed MCMV (*n*=6; average lesion size 89,928±13,700 μ^2; $p<0.05$ compared to lesions in mice infected with live MCMV); **c** Lesions in aortas of mice infected with a live MCMV (*n*=8); **d** lesion area (μm^2±STD) in aortas of MCMV-infected vs. uninfected Apo E KO mice. Values represent average of *n*=8 mice (MCMV-infected and uninfected), $p=0.038$. *Arrows* show atherosclerotic lesions